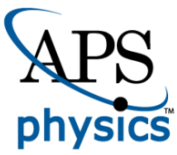

Physical Realization of Elastic Cloaking with a Polar Material

Xianchen Xu, Chen Wang, Wan Shou, Zongliang Du, Yangyang Chen, Beichen Li, Wojciech Matusik, Nassar Hussein, and Guoliang Huang

Phys. Rev. Lett. **124**, 114301 — Published 19 March 2020

DOI: 10.1103/PhysRevLett.124.114301

Physical Realization of Elastic Cloaking with a Polar Material

Xianchen Xu,[1†] Chen Wang,[1†] Wan Shou,[2,3†] Zongliang Du,[1,4] Yangyang Chen,[1] Beichen Li,[2,3]

Wojciech Matusik,[2,3] Nassar Hussein,[1]* & Guoliang Huang[1]*

[1] *Department of Mechanical and Aerospace Engineering, University of Missouri, Columbia, MO, USA*

[2] *Computer Science and Artificial Intelligence Laboratory, Massachusetts Institute of Technology, Cambridge, MA, USA*

[3] *Electrical Engineering and Computer Science Department, Massachusetts Institute of Technology, Cambridge, MA, USA*

[4] *Department of Engineering Mechanics, Dalian University of Technology, Dalian, 116023, P.R. China*

An elastic cloak is a coating material that can be applied to an arbitrary inclusion to make it indistinguishable from the background medium. Cloaking against elastic disturbances, in particular, has been demonstrated using several designs and gauges. None, however, tolerate the coexistence of normal and shear stresses due to a shortage of physical realization of transformation-invariant elastic materials. Here, we overcome this limitation to design and fabricate a new class of polar materials with a distribution of body torque that exhibits asymmetric stresses. A static cloak for full two-dimensional elasticity is thus constructed based on the transformation method. The proposed cloak is made of a functionally graded multi-layered lattice embedded in an isotropic continuum background. While one layer is tailored to produce a target elastic behavior, the other layers impose a set of kinematic constraints equivalent to a distribution of body torque that breaks the stress symmetry. Experimental testing under static compressive and shear loads demonstrate encouraging cloaking performance in good agreement with our theoretical prediction. The work sets a precedent in the field of transformation elasticity and should find applications in mechanical stress shielding and stealth technologies.

The artificially structured materials, known as metamaterials, have significantly improved our ability to steer waves and channel energy in different areas of physics [1-4]. In particular, they brought the invisibility cloaks, featured in several pop cultural landmarks, to reality. Briefly, a cloak is a coating material that makes an object indistinguishable from its surroundings or undetectable by external field measurements of a specific kind [5-6]; To name a few, invisibility cloaks for light [7,8], sound [9], heat [10] and so on [11-15]. In the years following their theorization, a number of experimental demonstrations of cloaking have been reported including cloaking against electromagnetic waves at microwave and optical frequencies [16], acoustic waves [17-20], surface waves in water [21], electric [22-24] and heat currents [25, 26], as well as flexural waves in thin elastic membranes and plates [27, 28]. Cloaking is achieved with transformations that deform a region in such a way that the mapping is one-to-one everywhere except at a single point, which is mapped into the cloak inner boundary. A key step in a cloak's design is to apply a suitable warping transformation to the background medium and to accordingly rewrite its governing equations in a manner that reveals what constitutive materials are needed. The constitutive parameters of the cloaking material in the physical domain can then be defined by a spatial transformation and gauge matrices. Often, these materials are anisotropic when the background medium is isotropic. At first sight, this should mean that cloaking in solids for full elasticity [28-30] is more accessible than in fluids for acoustics [32-34] since anisotropic solids are potentially easier to fabricate than "anisotropic fluids". Nonetheless, a closer look reveals that elastic cloaks, in general, further require their materials to be polar, i.e., to exhibit asymmetric stresses [35-40]. Polarity turns out to be necessary if shear and hydrostatic stresses are coupled as is typically the case in elasticity [37]. The lack of subwavelength microstructures, whose unit cell size is much smaller than operating wavelength, producing an effective polar elastic behavior has blocked the progress in the area of cloaking in solids for decades. Here, we propose a new way to fabricate and test the first of these structures for cloaking applications in two dimensional elasticity.

It has long been thought that the Cosserats' micropolar solids are suitable for cloaking given that they naturally feature asymmetric stresses [35]. This common wisdom is misleading, however, since what truly distinguishes the Cosserat theory from the standard one by Cauchy, kinetically and kinematically, is the presence of couple stresses on one hand and of microrotations on the other hand instead of the nature of the Cauchy stress tensor. This observation has led us, within the standard theory, to revisit the principle responsible for the symmetry of stresses, namely the local balance of angular momentum. It then becomes clear that achieving cloaking in solids by breaking the stress symmetry relies on finding the structures where

†Contributed equally

*Email: nassarh@missouri.edu; huangg@missouri.edu

the balance of angular momentum is maintained differently. In what follows, we physically realize that by introducing the distribution of large body torques in the form of constraints which limit the local rotations [37]. We propose a design of a metamaterial with several layers, one to guide stresses, and the others to impose the constraints. Tests performed under static compression and shear demonstrate satisfactory cloaking performance of a semi-circular void or inclusion. We hope that the present contribution will fill the current gap which separates the transformation elasticity, in both static and dynamic regimes, from the already mature fields of transformation acoustics and optics thus enabling similar capabilities in the control and steering of general stress fields.

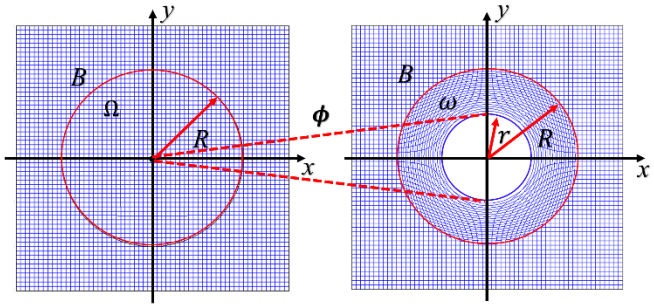

FIG. 1. Schematic representation of the transformation method: $\boldsymbol{\Omega}$ is a fictitious reference medium and $\boldsymbol{\omega}$ is the physical medium; transformation $\boldsymbol{\phi}$ maps a point of the reference into a circular area of radius r hosting the cloaked object while leaving unchanged the background beyond a distance R from the center; the remaining annulus of thickness $R-r$ hosts the cloak.

Consider the two media $\boldsymbol{\Omega}$ and $\boldsymbol{\omega}$ of Fig. 1: the former is a fictitious reference medium and the latter is the physical medium. While they match in shape and composition over the background $\boldsymbol{B}$, they differ within a disk of radius R corresponding to a cloaked area, which is composed of a cloak of thickness $R-r$ and of a cloaked circular object of radius r. Cloaking is successful when the respective displacement fields $\boldsymbol{U}$ and $\boldsymbol{u}$ of $\boldsymbol{\Omega}$ and $\boldsymbol{\omega}$ are equal over the background B regardless of the applied loading or of the composition of the cloaked object. To derive the elastic properties of the cloak, we ensure that $\boldsymbol{\Omega}$ and $\boldsymbol{\omega}$ have elastic energy densities $\mathcal{L}(\boldsymbol{\nabla U}) = C_{ijkl}U_{i,j}U_{k,l}/2$ and $\ell(\boldsymbol{\nabla u}) = c_{ijkl}u_{i,j}u_{k,l}/2$ that are identical up to the change of variables $\boldsymbol{U}(\boldsymbol{X}) = \boldsymbol{u}(\boldsymbol{x})$ for $\boldsymbol{x} = \boldsymbol{\phi}(\boldsymbol{X})$ where $\boldsymbol{\phi}$ maps $\boldsymbol{\Omega}$ to $\boldsymbol{\omega}$. That is $\ell(\boldsymbol{\nabla u}) = \mathcal{L}(\boldsymbol{\nabla u F})/J$ or in terms of elasticity tensors: $c_{ijkl} = J^{-1}F_{jm}F_{ln}C_{imkn}$, $\boldsymbol{F} = \boldsymbol{\nabla\phi}$, and $J = |\boldsymbol{F}|$ [36]. In what follows, the background $\boldsymbol{B}$ is assumed to be homogeneous and isotropic; the cloaked object is a void; and the cloaking transformation is radially symmetric: $\boldsymbol{x} = \frac{f(r)}{\|\boldsymbol{X}\|}\boldsymbol{X}$ with $f(r) = (\|\boldsymbol{x}\| - r)/\|\boldsymbol{x}\|$, where the radius r is measured from the center of the cloaked area.

Therefore, cloaking an object in a background $\boldsymbol{B}$ of elasticity tensor $\boldsymbol{C}$ requires materials whose elasticity tensor is $\boldsymbol{c}$; the problem is that no such materials are known. As a matter of fact, standard elasticity tensors satisfy three fundamental properties: (*i*) they are positive definite, namely if $\boldsymbol{E}$ is non-skew then $C_{ijkl}E_{ij}E_{kl} > 0$; (*ii*) they have the major symmetry $\boldsymbol{C}_{ijkl} = \boldsymbol{C}_{klij}$ and (*iii*) the minor symmetry $\boldsymbol{C}_{ijkl} = \boldsymbol{C}_{ijlk}$. By analyzing the constitutive behavior of the transformed/coating material in the Brun–Guenneau–Movchan (BGM) gauge [1], we found that $\boldsymbol{c}$ only satisfies condition (*ii*) of major symmetry [37, 38]. We come to conclude that cloaking materials, were they to exist, must accommodate a compliant mechanism, i.e., a zero-energy deformation mode or "zero mode". In the present case, the zero mode is $\boldsymbol{E}_{zm} = f(r)\boldsymbol{e}_1 \otimes \boldsymbol{e}_2 - \boldsymbol{e}_2 \otimes \boldsymbol{e}_1$ (detailed derivation in Appendix B). As for condition (*iii*), it is a consequence of Cauchy's second law of motion stating that the skew part of the stress tensor is equal to the externally applied body torque: $t = \epsilon_{3jk}\sigma_{jk} = \sigma_{12} - \sigma_{21}$. Typically, body torque is zero, the stress tensor is symmetric and the elasticity tensor has minor symmetry. Negating the latter, we deduce that cloaking materials are necessarily a polar material, a material that elastically resists rotation, and must be subject to an externally applied body torque $t = \mu[\left(\frac{1}{f} - 1\right)E_{12} - (f-1)E_{21}]$ with $E_{ij} = U_{i,j}$ [37,38].

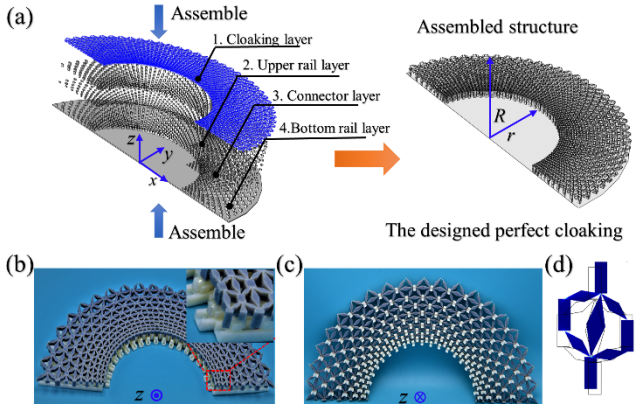

FIG. 2. The design and fabrication of the polar-mechanical perfect cloak. (a) The cloak consists of 4 different layers, in the z-axis view, from top to bottom, which is arranged as: layer 1-cloaking lattice; layer 2-upper rail; layer 3-connector; and layer 4-bottom rail. The bottom rail layer is fixed in a rigid plate as a ground condition.The size cloaking region and cloaking lattice are r=95 mm and R = 200 mm respectively. Any object can be placed inside of the hollow interior and thereby becomes 'unfilmable'. For any given pulling direction, the cylindrical core-shell geometry exhibits a symmetry plane normal to the pushing direction and cutting through the middle of the cylinder. Thus, it is sufficient to study the half-cylinder geometry. (b) The top view of the assembled cloak. The layer 1 (cloaking lattice) has been assembled with layer 2, layer 3 and layer 4. (c) The bottom view reveals the details of the polar-mechanical perfect cloak, the blue

lattice is layer 1, and the white part is layer 2. (d) Illustration of zero-mode of the unit cell of cloaking layer.

In this study, we design and fabricate a new class of cloaking (polar) materials based on the transformation method. The cloaking material is composed of a functionally graded four-layered lattice embedded in an isotropic continuum background as shown in Figs. 2(a)-(c). A mechanism to make interconnection among the four layers is proposed: layer 1 (cloaking layer) works as the lattice guiding the stresses; layer 2 (upper rail layer) is the first set of rails whereas, layer 4 (bottom rail layer) is the second set of rails bound to a relatively rigid material as an effective ground; layer 3 (connector layer) connects layer 2 and layer 4 and ensures the transmission of torques between them as shown in Fig. 2(a). In our design, each lattice site is free to move by sliding over an assembly of two orthogonal rails. By grounding the rails, the sites' rotations are impeded. In other words, the grounded rails act as a torsional spring: they apply a torque proportional to the site's angle of rotation. (Detailed in Appendix A). As a result, the distributed external torques t are properly applied to break stress symmetry. Given that, the lattice material shown in Figs. 2(b) and (c) exhibit an effective elasticity tensor of the same form as $\boldsymbol{c}$. At each location x, the thickness of the bars and the aspect ratio of the unit cell must be adjusted to fit exactly the targeted tensor $\boldsymbol{c}$; this is confirmed for each unit cell through a numerical homogenization procedure. Meanwhile, the thickness of the hinges is kept to a minimum to approximately reproduce the behavior of an ideal pin transmitting zero bending moment. Therefore, the zero mode of the lattice shown in Figure 2 (d) can be easily obtained by adjusting the geometrical relations among the bars as tension-compression elements (Detailed in Appendix B).

The layers were 3D printed and manually assembled; the material properties are listed in Table 1 [41,42]. It is noteworthy that the Poisson's ratio of the background medium is 0.33; in this particular case, the elastic moduli of the rails, connectors, and ground become irrelevant as long as they are significantly higher than those of the background. For other Poisson's ratios, these moduli become important design parameters. To validate our design strategy, numerical simulations of a void cloaked in a two-dimensional plate under either pressure or shear loading are conducted by using a fictitious polar continuum and then by using the proposed lattice-based medium; the comparison showed very good agreement (Details in Appendix C). In the simulation, we also demonstrate the displacement fields in the proposed lattice structures with and without body torque and the excellent elastic cloaking performance from the polar material.

Table.1 Material properties of the designed cloaking

	Young's modulus (GPa)	*Density(kg/m^3)*	*Poisson's ratio*
Layer 1	1.50	1170	0.33
Layer (2~4)	2.50	1180	0.33
Host medium	1.25	1270	0.33

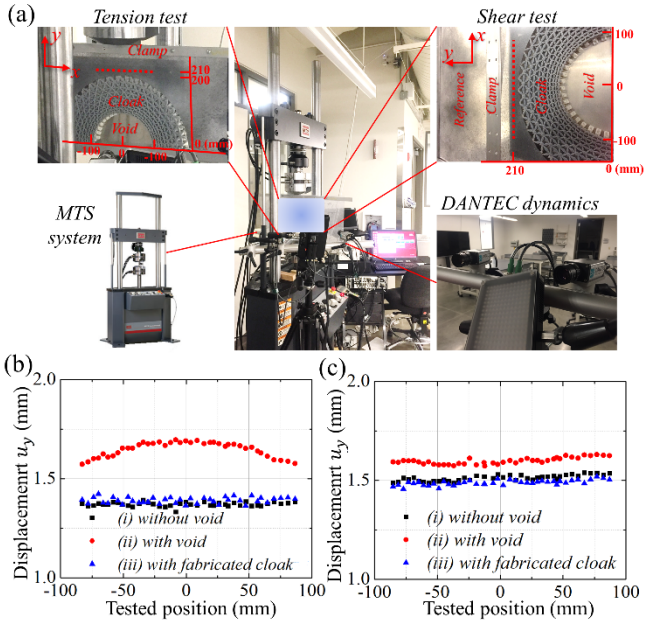

FIG. 3. (a) The experimental setup of both tension and shear static test of the elastic cloak. The sample consists of lattice cloak, background material, void, and clamp. The tension and shear loading are supplied by the MTS system. The displacement in dotted red line due to the strain is measured by DANTEC dynamics system (The width of the dotted red line is from -100 mm to 100 mm in the x-axis and the distance from the measured line to the bottom of the plate is 210mm in the y-axis); (b) Measured displacement fields with and without the cloaking device under a static pressure field applied to the top boundary and fixed boundary conditions from below: (*i*) without void (black squares), (*ii*) with void (red dots), (*iii*) with fabricated cloak (blue triangles). (c) Measured displacement fields with and without the cloaking device under a static shear field applied to the center of the plate and fixed boundary conditions on the other side: (*i*) without void (black squares), (*ii*) with void (red dots), (*iii*) with fabricated cloak (blue triangles).

To test its cloaking abilities, the proposed design is bonded to a background medium through its stress guiding layer, i.e., layer 1. In the quasi-static characterization experiments shown in Fig. 3(a), a holder holds the top side of the sample and pull onto the sample via a motorized translational stage [43]. The loading is applied by an MTS system both for tension and shear tests. The loading speed is 0.2 mm/min. To keep the deformations in the linear region, we apply a maximum global strain of about 1%. The holder at the bottom is fixed. In the tested sample, the void is a half circle with a radius of 95 mm and the radial thickness of the lattice cloak is 200 mm attached to the host medium plate with a length of 300 mm and a width of 600

mm. Meanwhile, the backside of layer 4 is fixed to an aluminum plate with length 400 mm and width 250 mm. We optically image the entire structure from the side, that is, in a plane perpendicular to the sample, and film the deformation using a DANTEC dynamics system while varying the loading. The obtained images are analyzed using an autocorrelation software tracking individual points (red dotted line in experimental setup) and delivering a spatial resolution beyond that of the individual camera pixels. This analysis provides us with the displacement directly from the experiment with a good signal-to-noise ratio. In this manner, the background medium is loaded and displacements are measured in two cases pertaining to tension and shear. The measurements are then compared to those obtained by loading two reference samples of the background medium, one with the void and one without it, both in the absence of the cloak.

The measured displacements are depicted in Figs. 3(b) and (c) for the tension test and the shear test, respectively. Both plots show satisfactory cloaking performance. In particular, the lattice cloak succeeds in suppressing the localization expected and observed in the vicinity of the uncloaked void and restores the uniform displacement profile observed in the reference sample. In other words, the cloak reinforces the void without disturbing the fields in the background. Comparison of numerical (Appendix C) and experimental results is satisfactory as well: the minor differences observed could be attributed to the variability of the material properties produced by the 3D printing of both the lattice cloak and the host medium.

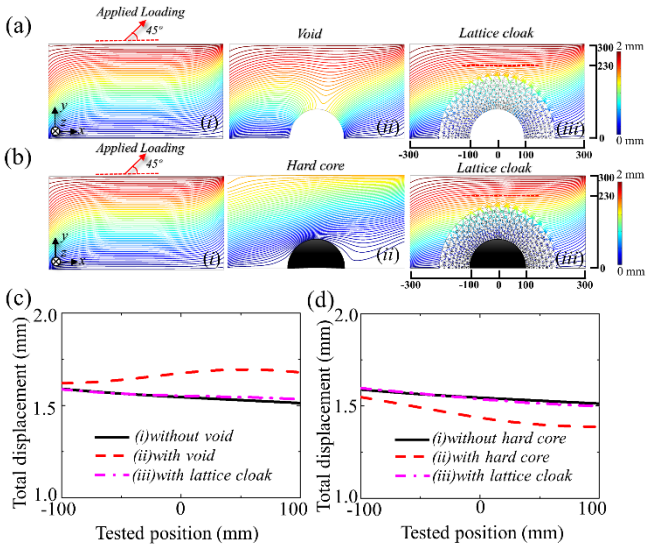

FIG. 4. The total displacement field under a general mechanical loading (red arrow) at the top boundary of the test plate has been shown: (a) (*i*) without void, (*ii*) with void, (*iii*) with lattice cloak; (b) (*i*) without hard core, (*ii*) with hard core, (*iii*) with lattice cloak. The total displacement at dotted line (see *iv*, from -100 mm to 100 mm in the *x*-axis, at 230 mm in the *y*-axis) for plate with void and hard core have been shown in (c) and (d) respectively.

Coated inclusions that do not disturb background fields obtained under loading at infinity are known as "neutral inclusions" [44,45]. Typically, however, the properties of the coating need to be changed in function of the loading and of the core's properties. By contrast, the proposed cloak is universal. On one hand, the provided experimental results, along with the isotropy and linearity assumptions, show that the tested loading can be combined and rotated so as to guarantee similar cloaking performance for any static loading. As an example, a mechanical cloaking is simulated in the presence of a localized force applied at a 45º angle to the top boundary with satisfactory results (Fig. 4(a)). On the other hand, based on the transformation method, it is possible to predict similar cloaking performance for any core properties (void, elastic or rigid). Indeed, the void's region is equivalent to a vanishingly small region, ideally a point, in the original domain. Therefore, filling the void with different material amounts to changing the elastic properties of a small region of the original medium; such a perturbation has negligible effects on any static equilibrium. Here too, numerical simulations validate this hypothesis: cloaking a hard core (aluminum) instead of a void, using the same lattice, produces the same fields in the background as those present in the absence of both inclusions (Fig 4.b-d).

In this study, we report on the design and fabrication of a static cloak shielding against combined pressure and shear stress fields using lattice-based polar materials that exhibit asymmetric stresses. We experimentally and numerically investigate the characteristics of the proposed cloak and find very good cloaking performance under both tension and shear loadings. The cloak is further universal in that it is able to hide an inclusion of arbitrary composition from external loadings of arbitrary orientation. Our results here, restricted to statics, will help make cloaking against stress waves and dynamic loadings experimentally accessible in the near future using similar polar materials-based architectures.

This work is supported by the Army Research Office under Grant No. W911NF-18-1-0031 with Program Manager Drs. David M. Stepp and Daniel Cole.

[1] M. Brun, S. Guenneau, and A. B. Movchan, Appl. Phys. Lett. **94**, 061903 (2009).
[2] G. W. Milton, *The Theory of Composites*, Cambridge University Press (2002).
[3] L. Solymar, and E. Shamonina, *Waves in metamaterials*. Oxford University Press (2009).
[4] J. B. Pendry, D. Schurig, and D. R. Smith, Science **312**, 1780 (2006).
[5] T. Bückmann, M. Kadic, R. Schittny, and M. Wegener, Proc. Natl. Acad. of Sci. USA **112**, 4930 (2015).
[6] H. Chen, and C. T. Chan, Appl. Phys. Lett. **91**, 183518 (2007).
[7] H. Chen, C. T. Chan, and P. Sheng, Nat. Mater. **9**, 387 (2010).

[8] U. Leonhardt, and T. Philbin, *Geometry and light: the science of invisibility*. Courier Corporation (2010).

[9] M. Farhat, S. Enoch, S. Guenneau, and , A. B. Movchan, Phys. Rev. Lett. **101**, 134501 (2008).

[10] R. Schittny, M. Kadic, S. Guenneau, and M. Wegener, Phys. Rev. Lett. **110**, 195901 (2013).

[11] G. W. Milton, M. Briane, and J. R. Willis, New J. Phys. **8**, 248 (2006).

[12] A. Diatta, and S. Guenneau, Appl. Phys. Lett. **105**, 021901 (2014).

[13] M. Farhat, S. Guenneau, and S. Enoch, Phys. Rev. Lett. **103**, 024301 (2009).

[14] M. Farhat, S. Guenneau, and S. Enoch, Phys. Rev. B. **85**, 020301 (2012).

[15] M. Farhat, S. Guenneau, S. Enoch, and A. B. Movchan, Phys. Rev. B. **79**, 033102 (2009).

[16] T. Ergin, N. Stenger, P. Brenner, J. B. Pendry, and M. Wegener, Science **328**, 337 (2010).

[17] S. A. Cummer, and D. Schurig, New J. Phys. **9**, 45 (2007).

[18] B. I. Popa, L. Zigoneanu, and S. A. Cummer, Phys. Rev. Lett. **106**, 253901 (2011).

[19] L. Sanchis, V. M. García-Chocano, R. Llopis-Pontiveros, A. Climente, J. Martínez-Pastor, F. Cervera, and J. Sánchez-Dehesa, Phys. Rev. Lett. **110**, 124301 (2013).

[20] S. Zhang, C. Xia, and N. Fang, Phys. Rev. Lett. **106**, 024301 (2011).

[21] S. Zou, Y. Xu, R. Zatianina, C. Li, X. Liang, L. Zhu, Y. Zhang, G. Liu, Q. H. Liu, H. Chen, and Z. Wang, Phys. Rev. Lett. **123**, 074501 (2019).

[22] M. Kadic, T. Bückmann, R. Schittny, and M. Wegener, Rep. Prog. Phys. **76**, 126501 (2013).

[23] F. Yang, Z. L. Mei, T. Y. Jin, and T. J. Cui, Phys. Rev. Lett. **109**, 053902 (2012).

[24] J. Andkjær, and O. Sigmund, Appl. Phys. Lett. **98**, 021112 (2011).

[25] H. Xu, X. Shi, F. Gao, H. Sun, and B. Zhang, Phys. Rev. Lett. **112**, 054301 (2014).

[26] T. Han, X. Bai, D. Gao, J. T. Thong, B. Li, and C. W. Qiu, Phys. Rev. Lett. **112**, 054302 (2014).

[27] N. Stenger, M. Wilhelm, and M. Wegener, Phys. Rev. Lett. **108**, 014301 (2012).

[28] Y. Chen, X. Li, H. Nassar, G. Hu, and G. Huang, Smart Mater. Struct. **27**,115011 (2018).

[29] D. Misseroni, A. B. Movchan, and D. Bigoni, P. Roy. Soc. A **475**, 20190283 (2019).

[30] M. Kadic, M. Wegener, A. Nicolet, F. Zolla, S. Guenneau, and A. Diatta, Wave Motion **92**, 102419 (2020)

[31] X. Zhou, G. Hu, and T. Lu, Phys. Rev. B **77**, 024101 (2008).

[32] J. D. Smith, and P. E. Verrier, Proc. R. Soc. A **467**, 2291 (2011).

[33] M. Kadic, T. Bu¨ckmann, N. Stenger, M. Thiel, and M. Wegener, Appl. Phys. Lett. **100**, 191901 (2012).

[34] R. Schittny, T. Bu¨ckmann, M. Kadic, and M. Wegener, Appl. Phys. Lett. **103**, 231905 (2013).

[35] G. W. Milton, and A. Cherkaev, J. Eng. Mater. Technol. **117**, 483 (1995).

[36] A. N. Norris, and A. L. Shuvalov, Wave Motion, **48**, 525 (2011)

[37] H. Nassar, Y. Y. Chen, and G. L. Huang, J. Mech. Phys. Solids **129**, 229 (2019).

[38] H. Nassar, Y. Y. Chen, and G. L. Huang, P. Roy. Soc. A **474**, 20180523 (2018).

[39] Y. Achaoui, A. Diatta, M. Kadic, and S. Guenneau, Materials **13**, 449 (2020)

[40] M. Kadic, A. Diatta, T. Frenzel, S. Guenneau, and M. Wegener, Phys. Rev. B **99**, 214101 (2019)

[41] R. A. Brown, *Large strain deformation of PETG as processing temperatures* (Doctoral dissertation, Massachusetts Institute of Technology). (2000).

[42] http://www.padtinc.com/downloads/Stamp%20Digital%20Materials_Datasheet-08-13.pdf

[43] T. Bückmann, M. Thiel, M. Kadic, R. Schittny, and M. Wegener, Nat. Commun. **5**, 4130 (2014).

[44] Y. Chen, X. Liu, and G. Hu, J. Sound. Vib. **458**, 62 (2019).

[45] G. W. Milton, 2002 The theory of composites. Cambridge, UK: Cambridge University Press.